World Journal of Nano Science and Engineering, 2015, 5, 107-114
Published Online December 2015 in SciRes. http://www.scirp.org/journal/wjnse
http://dx.doi.org/10.4236/wjnse.2015.54013

Development of Nanostructure Formation of $Fe_{73.5}Cu_1Nb_3Si_{13.5}B_9$ Alloy from Amorphous State on Heat Treatment

Md. Khalid Hossain[1*], Jannatul Ferdous[2], Md. Manjurul Haque[2], A. K. M. Abdul Hakim[3]

[1]Institute of Electronics, Atomic Energy Research Establishment, Savar, Dhaka, Bangladesh
[2]Department of Applied Physics, Electronics & Communication Engineering, Islamic University, Kushtia, Bangladesh
[3]Department of Glass and Ceramic Engineering, Bangladesh University of Engineering and Technology, Dhaka, Bangladesh
Email: [*]khalid.baec@yahoo.com

Received 1 July 2015; accepted 7 October 2015; published 13 November 2015

Abstract

Iron-based amorphous alloys have attracted technological and scientific interests due to their excellent soft magnetic properties. The typical nanocrystalline alloy with the composition of $Fe_{73.5}Cu_1Nb_3Si_{13.5}B_9$ known as FINEMENT has been studied for structural properties analysis. Recently, it is found that after proper annealing the amorphous alloy like $Fe_{73.5}Cu_1Nb_3Si_{13.5}B_9$ has a transition to the nanocrystalline state, thus exhibiting good magnetic properties. The alloy in the form of ribbon of 10 mm width and 25mm thickness with the composition of $Fe_{73.5}Cu_1Nb_3Si_{13.5}B_9$ was prepared by rapid quenching method. The prepared ribbon sample has been annealed for 30 min in a controlled way in the temperature range 490˚C - 680˚C. By analyzing X-ray diffraction (XRD) patterns, various structural parameters such as lattice parameters, grain size and silicon content of the nanocrystalline Fe(Si) grains, crystallization behavior and nanocrystalline phase formation have been investigated. In the nanocrystalline state, Cu helps the nucleation of α-Fe(Si) grains while Nb controls their growth, Si and B has been used as glass forming materials. Thus on the residual amorphous, the nanometric Fe(Si) grains develops. From broadening of fundamental peaks, the optimum grain size has been determined in the range of 7 - 23 nm.

Keywords

Fe Based Alloy, Rapid Solidification, Crystallization Behavior, Nanocrystalline Phase Formation

[*]Corresponding author.

How to cite this paper: Hossain, M.K., Ferdous, J., Haque, M.M. and Hakim, M.A. (2015) Development of Nanostructure Formation of $Fe_{73.5}Cu_1Nb_3Si_{13.5}B_9$ Alloy from Amorphous State on Heat Treatment. *World Journal of Nano Science and Engineering*, **5**, 107-114. http://dx.doi.org/10.4236/wjnse.2015.54013

1. Introduction

A new class of iron based alloys was introduced in by Yoshizawa, Oguma and Yamauchi [1]. This novel material with the composition of $Fe_{73.5}Cu_1Nb_3Si_{13.5}B_9$ has a trade name FINEMENT. The particular about the new material is its ultrafine microstructure of bcc Fe-Si with the grain sizes of 10 - 15 nm that are due to the presence of Cu and Nb [1] [2] from which their soft magnetic properties derive lastly. The magnetic properties of $Fe_{73.5}Cu_1Nb_3Si_{13.5}B_9$ and related alloys were reported by many publications; here only some of the references are given [2]-[7].

Nanocrystalline materials constitute a new class of condensed matter having interesting properties, which are mostly microstructure dependent. These materials are first formed into amorphous ribbons and then annealed above the crystallization temperature to form the nanocrystalline microstructure that consists of bcc Fe(Si) nanograins embedded on amorphous matrix. The crystallization of Fe-Si-B amorphous ribbons contains 1 at.% Cu and 3 at.% Nb. The crystallization of bcc Fe(Si) solid solution from amorphous state takes place according to the basic scheme characteristic to the hypo-eutectic glasses [8]: am1→Fe(Si) + am2, where am1 and am2 are the initial amorphous precursor and the remainder amorphous phase respectively. There are mainly two phases in the alloys: a bcc Fe-Si solid solution and some residual amorphous phase. The average grain size of the bcc Fe(Si) phase is about 10 nm [2]. The addition of Cu and Nb results in the formation of an ultrafine grain structure [1] [2].

Recently, a generalization of the random anisotropy model, taking into account the two phase character of nanocrystalline materials, has been developed [9] and it explains the previously mentioned hardening as well as other features which cannot be understood without the generalization. Since the unique properties of nanostructured materials are dictated by the dimensions of the crystallites, it is very advantageous to control the size of the particles by controlling the annealing temperature of the specimens.

The aim of the present research work is to synthesize Fe-based alloys of $Fe_{73.5}Cu_1Nb_3Si_{13.5}B_9$ composition in the amorphous state by using rapid solidification technique and study their structural properties by varying the annealing condition. The annealing of Fe-based soft nanocomposite magnetic materials has been performed in air. X-ray diffraction technique has been used for the characterization of nanostructured phases.

2. Experimental

Rapid solidification technique was used to prepare the ribbons with composition $Fe_{73.5}Cu_1Nb_3Si_{13.5}B_9$. The amorphous ribbons ware prepared at a temperature 1500˚C in an argon atmosphere (0.2 to 0.3 atoms). The dimension of the ribbon was 10 mm width and 25 mm thickness. The purity of the material is Fe (99.98%), Cu (99+%), Nb (99.8%), Si (99.9%) and B (99.5%) as obtained from Johnson Mathey (Alfa Aesar Inc.). **Figure 1** shows the schematic diagram of melt spin system.

A PHILIPS PW3040 X′ Pert PRO X-ray diffractometer was used to study the crystalline phases of the prepared samples in the Materials Science Division, Atomic Energy Centre, Dhaka-1000, Bangladesh. The powder specimens were exposed to CuK_α radiation with a primary beam of 40 kV and 30 mA with a sampling pitch of 0.02˚ and time for each step data collection was 1.0 sec. A 2θ scan was taken from 10˚ to 90˚ to set possible fundamental peaks where Ni filter was used to reduce CuK_α radiation. All the data of the samples were analyzed using computer software "X' PERT HIGHSCORE". X-ray diffraction patterns were carried out to confirm the crystal structure. Instrumental broadening of the system was determined from θ - 2θ scan of standard Si. **Figure 2** and **Figure 3** show the X-ray diffraction technique and block diagram of the PHILIPS PW 3040 X′ Pert PRO XRD system respectively.

3. Results

To determine the crystalline phases, X-ray diffraction studies have been performed for samples annealed at different temperatures. **Figure 4** and **Figure 5** represent the X-ray diffraction spectra of quenched alloy and the alloy annealed at different temperatures for 30 min. In the figures, the parenthesis represents the indices of the reflecting planes of the phases. The bcc α-Fe(Si) phases are found, identified by using standard software. All the results of lattice parameter, grain size and silicon content at % for different annealing temperatures of composition are listed in **Table 1**.

In **Figure 6**, the lattice parameter of various annealed samples in the temperature range 490˚C - 680˚C have

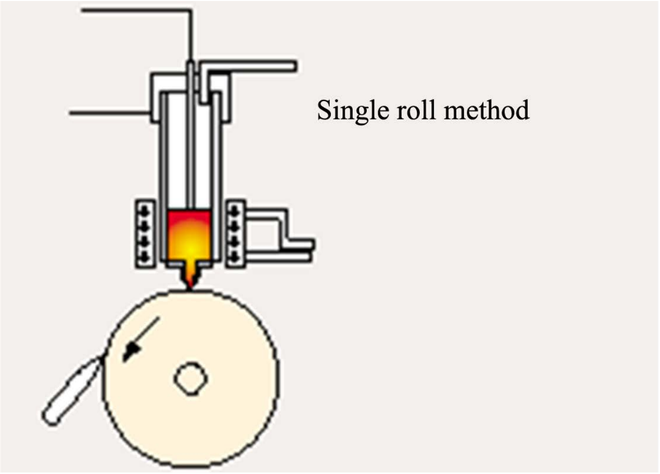

Figure 1. Schematic diagram of melt spin system.

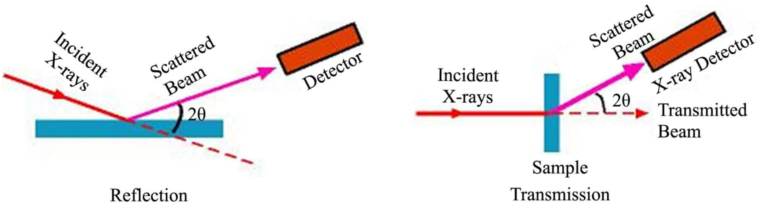

Figure 2. X-ray diffraction technique.

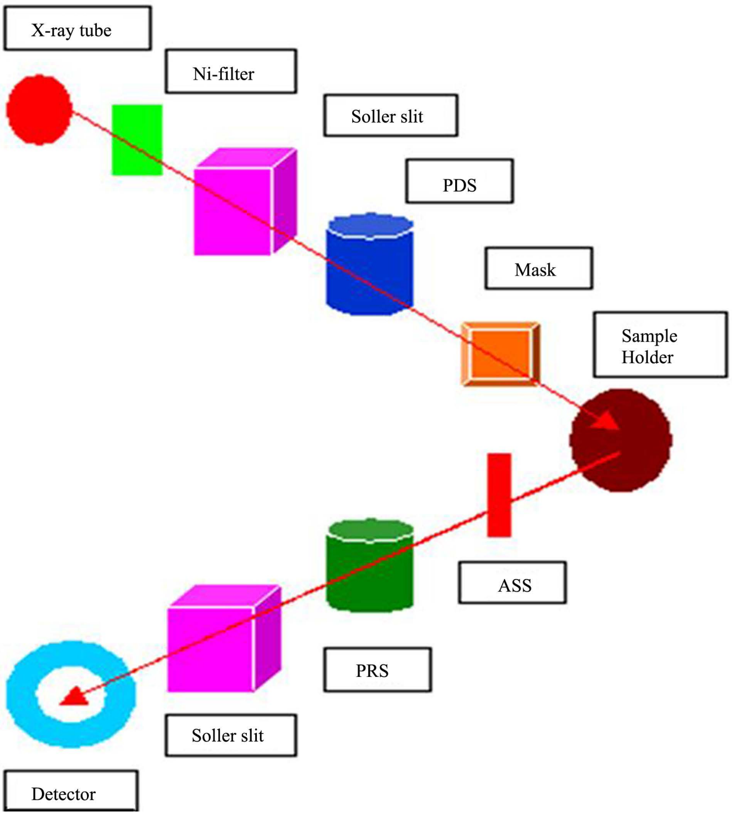

Figure 3. Block diagram of the PHILIPS PW 3040 X' Pert PRO XRD system.

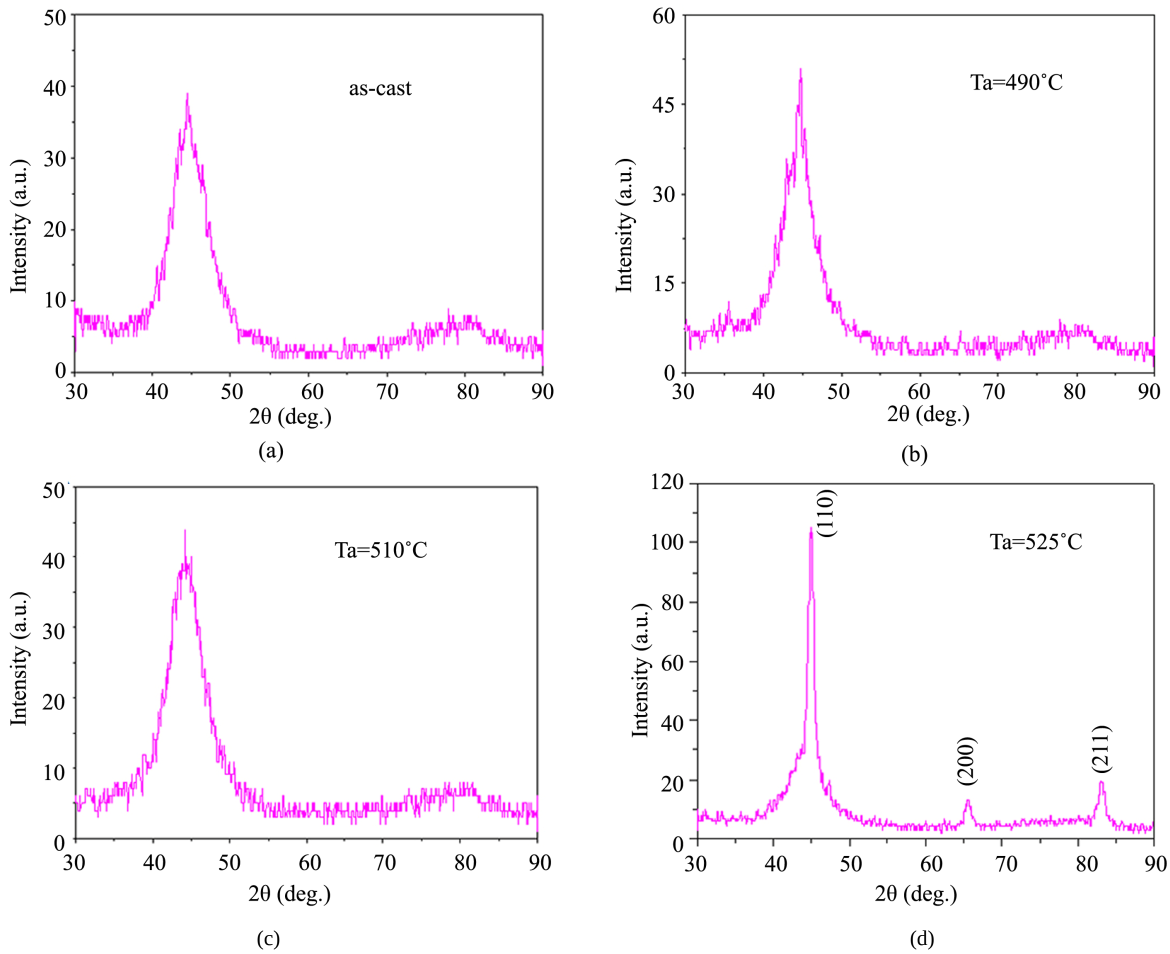

Figure 4. XRD patterns of $Fe_{73.5}Cu_1Nb_3Si_{13.5}B_9$ ribbon sample (a) as-cast and annealed samples at (b) 490˚C (c) 510˚C (d) 525˚C for 30 min.

Table 1. Experimental XRD data of nano-crystalline $Fe_{73.5}Cu_1Nb_3Si_{13.5}B_9$ amorphous ribbon at different annealing temperatures.

Annealing temperature, Ta (˚C)	Lattice parameter a_o (Å)	Grain size Dg (nm)	Silicon content (% Si)
As-cast	…	…	…
490	2.8615	7	6.45
510	2.8420	8	15.6
525	2.8373	10	17.8
545	2.8304	13	21.1
560	2.8307	14	20.8
600	2.8351	18	18.8
680	2.8482	23	12.7

been presented. In **Figure 6**, the established quantitative relationship [10] between lattice parameter was used to determine the silicon content of α-Fe(Si) nanograins. Nanocrystalline grain of α-Fe(Si) is formed from amorphous precursor, when the sample is annealed above the crystallization temperature. By using the Scherrer's formula, the mean grain size of the nanograins was determined from the X-ray fundamental line (110) has been presented in **Figure 8**.

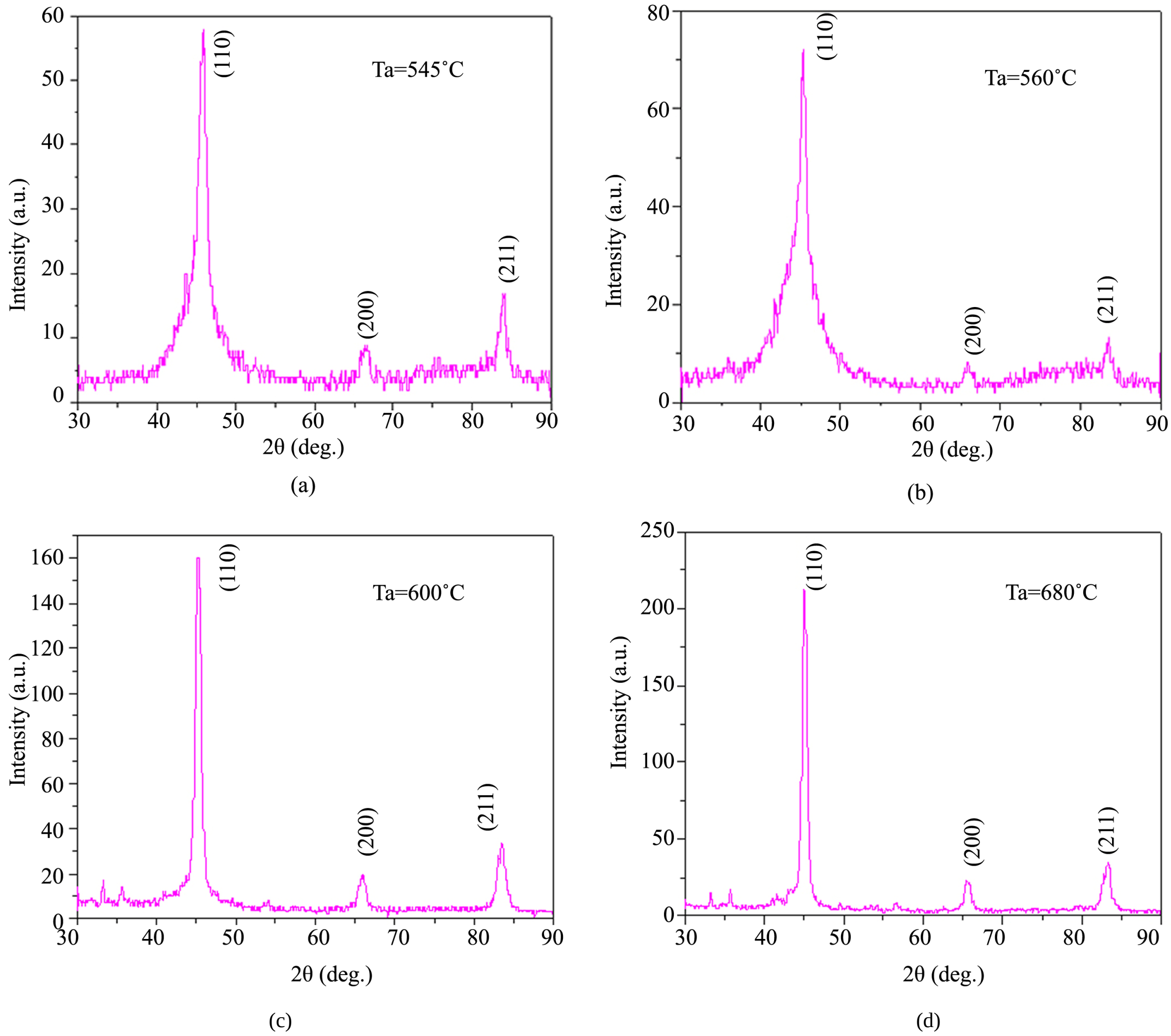

Figure 5. XRD patterns of $Fe_{73.5}Cu_1Nb_3Si_{13.5}B_9$ ribbon samples annealed at (a) 545˚C (b) 560˚C (c) 600˚C and (d) 680˚C for 30 min.

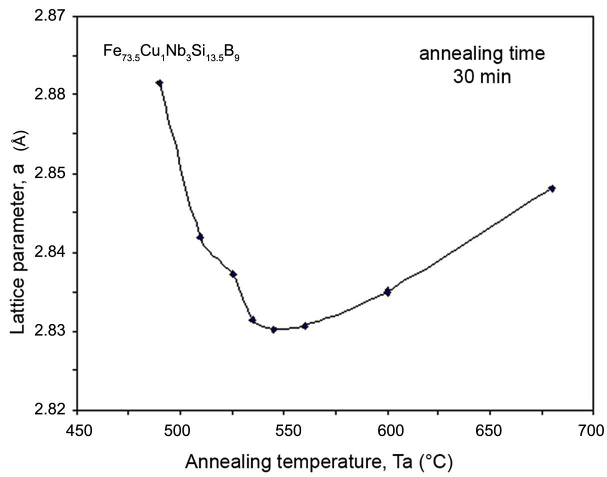

Figure 6. Variation of lattice constant with annealing temperature.

4. Discussion

Crystalline phases that developed through heat treatment have been studied by X-ray diffraction and presented in **Figure 4** and **Figure 5**. In the as cast condition the sample is in the amorphous state having no sharp peaks of crystalline phase since no crystalline phase have formed due to rapid quenching. When the sample is annealed above the crystallization temperature, nanocrystalline grain of *α*-Fe(Si) was formed in the amorphous precursor. X-ray diffraction results indicate that no *α*-Fe phases are present in the alloys annealed below 510˚C. The appearance of broader diffused pattern is also the characteristic of amorphous material was observed bellow the annealing temperature 510˚C. Crystalline phase was developed on the amorphous ribbon, when the alloys were annealed at or above 525˚C, which have been identified as a bcc *α*-Fe(Si) solid solution produced in the amorphous matrix. The peak of the bcc Fe phase in the alloys is increased with increasing of the annealing temperature of the crystalline nanograins of bcc Fe-Si phase was observed from the intensity of the diffraction lines in patterns obtained under the same conditions.

Figure 6 shows the lattice parameter of the bcc Fe-Si phase versus annealing temperature for the alloys. The lattice parameter of the bcc Fe-Si phase decreases with increasing annealing temperature up to 545˚C and then the value of lattice parameter increases up to annealing temperature 680˚C. It is observed that the lattice parameter slightly decreases with annealing temperature. It means that the silicon content in *α*-Fe(Si) alloy increases with annealing temperature since it is well known that the lattice parameter of bcc *α*-Fe(Si) alloys decreases with the increases of silicon content [11] [12]. Since the lattice parameter of *α*-Fe(Si) phases are always smaller than that of pure *α*-Fe, the value of which is 2.866 Å. Thus it can be assumed that the decrease of lattice parameter is due to the contraction of *α*-Fe lattice as a result of diffusion of the silicon with smaller atomic size into the iron lattice with larger atomic size forming a substitutional solid solution during the crystallization process to form *α*-Fe(Si). But the metalloid element B is practically insoluble in *α*-Fe (<< 0.01 at.%) and the solubilities [13] of Cu and Nb are low (< 0.2 at.% Cu, <0.1 at.% Nb only above 550˚C). Hence, the nanocrystalline phase consists essentially of Fe and Si.

In **Figure 7**, silicon content of *α*-Fe (Si) nanograins have been presented. A gradual increase of Si content in nanocrystalline phase with increasing annealing temperature is observed. This can be explained by the fact that the element Si from the amorphous phase diffuses into *α*-Fe space lattice by diffusion during the crystallization process to form *α*-Fe(Si) nanograins. This means that the crystallization behaviour of this material is a diffusion controlled process with temperature as controlling parameter. So the longer annealing temperature results in more diffusion of Si enriching the Fe(Si) nanograins. **Figure 8** shows the grain size increases gradually and attains a limiting value of 7 to 14 nm until 560˚C, which is very suitable for the exchange coupling through residual amorphous matrix [14]. A sudden increase of grain size above 650˚C is observed, achieving a value of 18 and 23 nm at 600˚C and 680˚C, respectively. Because annealing at higher temperature above 680˚C leads to the precipitation of Fe-borides [15]. The nanocrystalline material obtained in this way displays improved mechanical and magnetic properties in comparison to the ones achieved by conventional annealing [6] [16] [17].

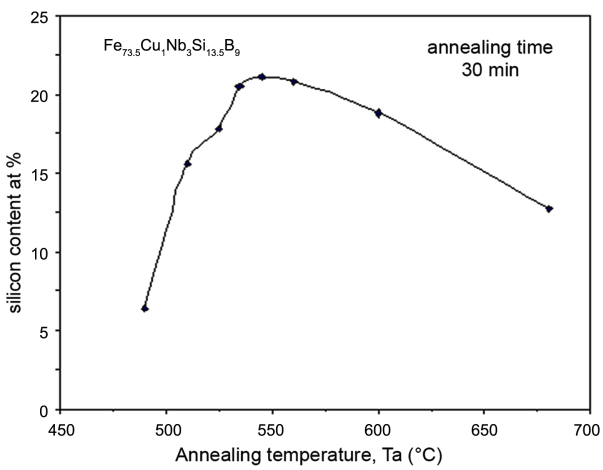

Figure 7. Variation of silicon content at.% with annealing temperature.

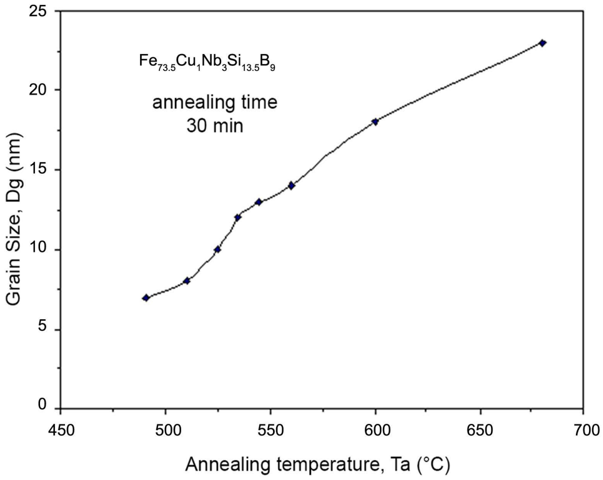

Figure 8. Average grain size as a function of annealing temperature.

5. Conclusion

X-ray diffraction results show that the grain size has been obtained in the range of 7 nm to 21 nm at different stage of annealing and Si content has been reached up to 21.1 at.%. The annealing of magnetic ribbon $Fe_{73.5}Cu_1Nb_3Si_{13.5}B_9$ at 545˚C for 30 min leads to the favorable nanocrystalline structure of bcc Fe(Si) mixed with a remaining amorphous fraction. The crystallization behavior of FINEMENT $Fe_{73.5}Cu_1Nb_3Si_{13.5}B_9$ is still an interesting subject of further research.

Acknowledgements

The authors are thankful to Materials Science Division, Atomic Energy Centre, Dhaka-1000, Bangladesh for providing the amorphous $Fe_{73.5}Cu_1Nb_3Si_{13.5}B_9$ ribbon materials and also for extending experimental facilities. We also thank Dr. Sheikh Manjura Hoque, Materials Science Division, Atomic Energy Centre, Dhaka-1000, for her valuable suggestions for the research work.

References

[1] Yoshizawa, Y., Oguma, S. and Yamauchi, K. (1998) New Fe-Based Soft Magnetic Alloys Composed of Ultrafine Grain Structure. *Journal of Applied Physics*, **64**, 6044. http://dx.doi.org/10.1063/1.342149

[2] Yoshizawa, Y. and Yamauchi, K. (1990) Fe-Based Soft Magnetic Alloys Composed of Ultrafine Grain Structure. *Materials Transactions*, **31**, 307. https://www.jim.or.jp/journal/e/31/04/307.html

[3] Yoshizawa, Y., Yamauchi, K., Yamane, T. and Sugihar, H. (1988) Common Mode Choke Cores Using the New Fe-Based Alloys Composed of Ultrafine Grain Structure. *Journal of Applied Physics*, **64**, 6047. http://dx.doi.org/10.1063/1.342150

[4] Yoshizawa, Y. and Yamauchi, K. (1989) Effects of Magnetic Field Annealing on Magnetic Properties in Ultrafine Crystalline Fe-Cu-Nb-Si-B Alloys. *IEEE Transaction on Magnetics*, **25**, 3324-3326. http://dx.doi.org/10.1109/20.42291

[5] Köster, U., Schünemann, U., Blank-Bewersdorff, M., Brauer, S., Sutton, M. and Stephenson, G.B. (1991) Nanocrystalline Materials by Crystallization of Metal-Metalloid Glasses. *Materials Science and Engineering*: *A*, **133**, 611-615. http://dx.doi.org/10.1016/0921-5093(91)90146-E

[6] Herzer, G. (1989) Grain Structure and Magnetism of Nanocrystalline Ferromagnets. *IEEE Transaction on Magnetics*, **25**, 3327. http://dx.doi.org/10.1109/20.42292

[7] Hilzinger, H.R. (1990) Recent Advances in Rapidly Solidified Soft Magnetic Materials. *Journal of Magnetism and Magnetic Materials*, **83**, 370-374. http://dx.doi.org/10.1016/0304-8853(90)90552-2

[8] Lovas, A., Kiss, L.F., Varga, B., Kamasa, P., Balogh, I. and Bakonyi, I. (1998) Survey of Magnetic Properties during and after Amorphous-Nanocrystalline Transformation. *Journal de Physique IV*, **8**, 291-298. http://dx.doi.org/10.1051/jp4:1998268

[9] Hernando, A., Vázquez, M., Kulik, T., and Prados, C. (1995) Analysis of the Dependence of Spin-Spin Correlations on the Thermal Treatment of Nanocrystalline Materials. *Physical Review B*, **51**, 1381. http://dx.doi.org/10.1103/PhysRevB.51.3581

[10] Franco, V., Conde, C.F., Conde, A. and Kiss L.F. (2000) Superparamagnetic Behaviour in an $Fe_{76}Cu_1Nb_3Si_{10.5}B_{9.5}$ Alloy. *Journal of Magnetism and Magnetic Materials*, **215-216**, 400-403. http://dx.doi.org/10.1016/S0304-8853(00)00170-0

[11] Zhi, J., He, K.-Y., Cheng, L.-Z. and Fu, Y.-J. (1996) Influence of the Elements Si/B on the Structure and Magnetic Properties of Nanocrystalline $(Fe,Cu,Nb)_{77.5}Si_xB_{22.5-x}$ Alloys. *Journal of Magnetism and Magnetic Materials*, **153**, 315-319. http://dx.doi.org/10.1016/0304-8853(95)00548-X

[12] Yoshizawa, Y., Oguma, S. and Yamauchi, K. (1958) A Handbook of the Lattice Spacing and Structure of Metals and Alloys. Pergamon, London, 6044.

[13] Kubaschewski, O. (1982) Iron-Binary Phase Diagrams. Springer Verlag, Berlin, Heidelberg. http://link.springer.com/book/10.1007%2F978-3-662-08024-5

[14] Herzer, G. (1997) Nanocrystalline Soft Magnetic Alloys. In: Buchow, K.H.J., Ed., *Handbook of Magnetic Material*, Vol. 10, Elsevier B.V., Amsterdam.

[15] Allia, P., Baricco, M., Knobel, M., Tiherto, P. and vanai, F. (1994) Soft Nanocrystalline Ferromagnetic Alloys with Improved Ductility Obtained through dc Joule Heating of Amorphous Ribbons. *Journal of Magnetism and Magnetic Materials*, **133**, 243-247. http://dx.doi.org/10.1016/0304-8853(94)90536-3

[16] Dahlgren, M., Grössingera, R., Hernandob, A., Holzera, D., Knobelc, M. and Tibertod, P. (1996) Magnetic Properties of $Fe_{86}Zr_7Cu_1B_6$ at Elevated Temperatures. *Journal of Magnetism and Magnetic Materials*, **160**, 247-248. http://dx.doi.org/10.1016/0304-8853%2896%2900180-1

[17] Herzer, G. (1990) Grain Size Dependence of Coercivity and Permeability in Nanocrystalline Ferromagnets. *IEEE Transaction on Magnetics*, 2**6**, 1397-1402. http://dx.doi.org/10.1109/20.104389